

Analysis of Ionospheric Scintillations using GPS and NavIC Combined Constellation

Shiva Kumar Nimmakayala

Department of EECE, GITAM School of Technology, GITAM Deemed to be University, India
121960402502@gitam.in (corresponding author)

Bala Sai Srilatha Indira Dutt Vemuri

Department of EECE, GITAM School of Technology, GITAM Deemed to be University, India
svemuri@gitam.in

Received: 17 March 2023 | Revised: 19 April 2023 | Accepted: 21 April 2023

Licensed under a CC-BY 4.0 license | Copyright (c) by the authors | DOI: <https://doi.org/10.48084/etasr.5863>

ABSTRACT

The disturbances and irregularities in the ionosphere are the primarily recognized ramifications of space weather called scintillations. Irregularities in the electron densities are the source of the ionospheric scintillations. This article investigates the ionospheric scintillations, which are predominant in the trans-equatorial and equatorial regions. Based on the data from a multi-constellation Global Navigation Satellite Systems (GNSS) receiver at the Chaitanya Bharathi Institute of Technology Hyderabad, the relationship between the amplitude scintillation index S_4 and the rate of change of total electron content (ROTI) is examined. The correlation coefficient between S_4 and ROTI is demonstrated in this article. The outcome validates the usefulness of the ROTI in identifying the scintillations.

Keywords-ionospheric scintillations; rate of change of total electron content; amplitude scintillation index; Global Navigation Satellite System (GNSS)

I. INTRODUCTION

The advancement of the Global Navigation Satellite System (GNSS), which encompasses GLONASS, GPS, BeiDO, Galileo, and numerous regional navigation systems, directed advanced steps in the earth's atmosphere research [1]. The space-based investigation of the GNSS signals is one of best enforced ways to investigate the ionosphere [2]. The space weather trans-ionospheric signals can undergo expeditious variations and disturbances both in amplitude and phase when they pass through indiscriminate electron density irregularities which are present in the ionosphere [3-4]. This anomaly is generally referred to as ionospheric scintillations. The temporal and spatial status of the ionospheric scintillations depends on geographical and geophysical locations, the time of the day, and season [5-6]. The ionospheric scintillations are the major sources of degradation of the VHF band and C band signals, immensely effecting navigation and communication systems [7]. Hence, it is vital to investigate and analyze them. The GNSS signals are considered a robust tool to investigate the Total Electron Content (TEC) and the existence of ionospheric scintillations [8]. Phase and amplitude scintillations are both ionosphere irregularities.

II. GNSS DATA COLLECTION

For this analysis, the data of the multi constellation GNSS receiver of Chaitanya Bharati Institute of Technology, which is located in Hyderabad, during the period from 2020-06-07 to

2020-06-13 were taken into account. The considered parameters are time, PRN (Pseudo Random Number) of the satellite, carrier to noise values of the received signal, and the ionospheric delay of the received signal. To reduce complexity, only the results of 2020-06-07 are shown in this paper.

III. METHODOLOGY

The ionospheric irregularities and scintillations can be investigated in two ways when using GNSS signals. The first of these methods uses carrier to noise (C/N_0) ratio to calculate the amplitude scintillation index S_4 [9] and the second one uses ionospheric delay to calculate the rate of change of TEC index (ROTI) which is the replacement index of S_4 [10]. The current work is based on the multi-step interpretation and processing of the L_1 (1575.42MHz), L_5 (1176.45MHz), and S_1 (2492.028MHz) GNSS signals corresponding to GPS and NavIC satellite constellations.

In the first method, the amplitude scintillation index S_4 is calculated as the ratio of the standard deviation to the mean value of the averaged C/N_0 [9]. The effectiveness of the amplitude scintillations index is divided into 3 categories which are weak scintillations when S_4 is less than 0.3, moderate scintillations when S_4 ranges between 0.3 and 0.6, and strong scintillations when S_4 is above 0.6 [11]. The amplitude scintillations are calculated as follows:

$$S_4 = \sqrt{\frac{\langle SI^2 \rangle - \langle SI \rangle^2}{\langle SI \rangle^2}} \quad (1)$$

where SI is the intensity of the received trans-ionospheric signal. The S_4 value is computed using the signals received on the L_1 (1575.42MHz), L_5 (1176.45MHz) and S_1 (2492.028MHz) frequencies for a week-long data from 2020-06-07 to 2020-06-13.

The second method is to calculate the ROTI using the delay due to ionosphere in the received signals [12]. The ionospheric delay is computed by:

$$ID_{ion} = \frac{40.3}{f^2} * TEC \quad (2)$$

where TEC indicates the Total Electron Content on the frequency of the received trans-ionospheric signal and ID_{ion} is the ionospheric delay of the received signal. TEC is used to describe all the electrons that are present along the path from the satellite to the receiver [12-13]. The TEC is expressed below and is measured in TECU:

$$1 \text{ TECU} = 10^{16} \text{ e/m}^2 \quad (3)$$

$$TEC = \frac{ID_{ion} * f^2}{40.3} \quad (4)$$

The rate of change of TEC (ROT) is calculated at regular intervals by (5):

$$ROT = \frac{TEC_b^a - TEC_{b-1}^a}{t_b - t_{b-1}} \quad (5)$$

where b specifies the epoch time and a specifies the noticeable satellite.

ROTI is calculated by the standard deviation of ROT:

$$ROTI = \sqrt{\langle ROT^2 \rangle - \langle ROT \rangle^2} \quad (6)$$

The effectiveness of ROTI is divided into three categories: It is fragile when the ROTI index ranges between 0.25 and 0.5, modest when the ROTI index ranges between 0.5 and 1, and vigorous when the ROTI index is above 1 [14-15]. ROTI was calculated for signals received on L_1 , L_5 , and S_1 frequencies for a weak long data from 2020-06-07 to 2020-06-13. To observe the correlation between ROTI and S_4 , the covariance and standard deviation of S_4 and ROTI are computed [16] by:

$$\sigma_{S_4} = \sqrt{\langle S_4^2 \rangle - \langle S_4 \rangle^2} \quad (7)$$

$$\sigma_{ROTI} = \sqrt{\langle ROTI^2 \rangle - \langle ROTI \rangle^2} \quad (8)$$

The covariance of S_4 and ROTI is:

$$C_{1ROTI S_4} = \sum_0^N \frac{(S_4 - \bar{S}_4)(ROTI - \bar{ROTI})}{N} \quad (9)$$

where \bar{S}_4 is the mean of S_4 and \bar{ROTI} is the mean of ROTI.

The correlation coefficient is a measure of the correlation between ROTI and S_4 methods which is expressed by $\rho_{1ROTI S_4}$, and it is given as:

$$\rho_{1ROTI S_4} = \frac{C_{1ROTI S_4}}{\sigma_{1ROTI} \sigma_{S_4}} \quad (10)$$

where $C_{1ROTI S_4}$ specifies the covariance of S_4 and ROTI.

The flowchart of the followed methodology is shown in Figure 1.

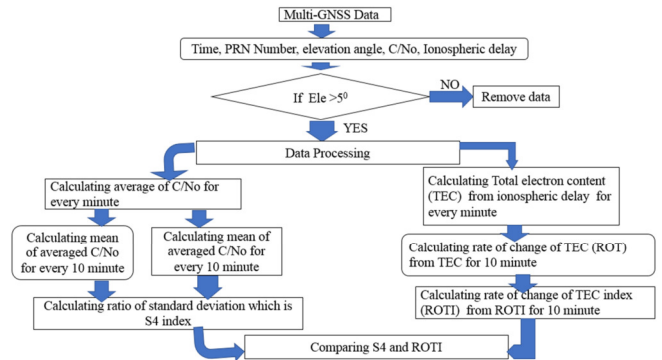


Fig. 1. Flowchart of the methodology.

IV. RESULTS AND DISCUSSION

The pseudo range measurements data of multi-constellation GNSS receiver, which were sampled every 1s, are considered for computation and analysis of amplitude scintillations, ROT, and ROTI. Figure 2 specifies S_4 for all the available satellites on 2020-06-07 for the L_1 frequency. The highest scintillations are observed from the satellite PRN 9. Therefore, the values of S_4 and ROTI are compared to the PRN 9 values.

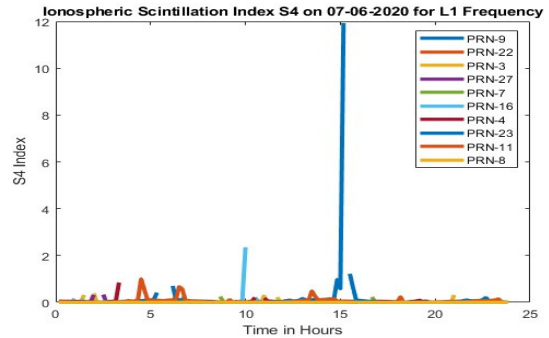


Fig. 2. S_4 index on 2020-06-07 for the L_1 frequency.

Figure 3 shows the comparison plot for S_4 and ROTI for the PRN-9, which exhibits maximum scintillations.

Figure 4 shows the correlation between ROTI and S_4 . The x axis specifies the epoch time for every hour and the y axis the correlation coefficient between S_4 and ROTI. The highest correlation coefficient is 1 and the minimum is higher than the cutoff level. As a result, the correlation coefficient is robust due to the persistent link between ROTI and S_4 . Figure 5 depicts the comparison of S_4 for all the available NavIC satellites on 2020-06-07 for the L_5 frequency. The maximum observed S_4 index is 0.0205 for IR-02, which is an indication of no scintillations on 2020-06-07 for the L_5 frequency. The highest S_4 values are observed in the IR-02 satellite. Therefore, the values of S_4 and ROTI are compared to the IR-02 values.

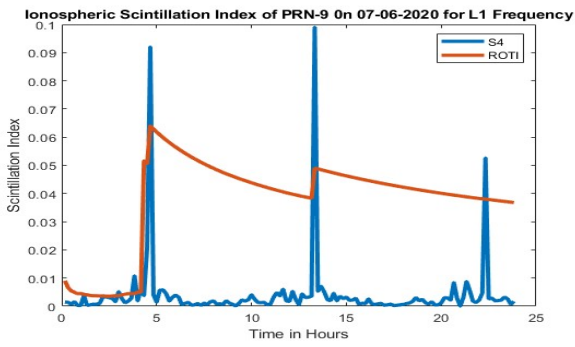


Fig. 3. Comparison of S_4 and ROTI on 2020-06-07 for PRN-9 (L_1 frequency).

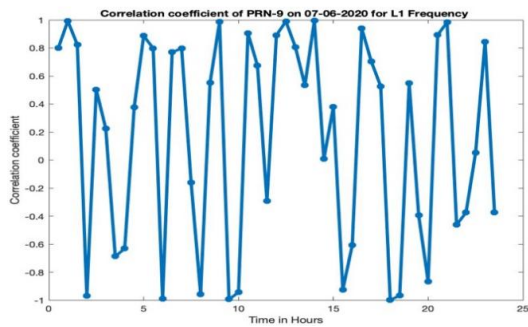


Fig. 4. Correlation of S_4 and ROTI on 2020-06-07 for PRN-9 (L_1 frequency).

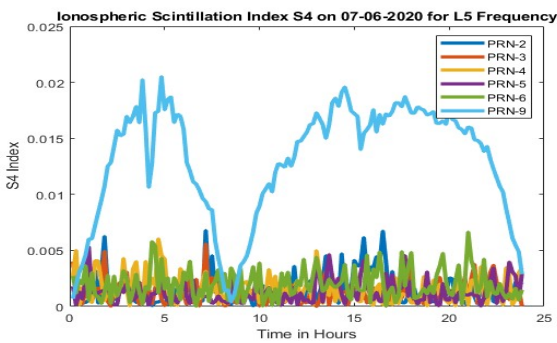


Fig. 5. S_4 amplitude variations on 2020-06-07 for L_5 frequency.

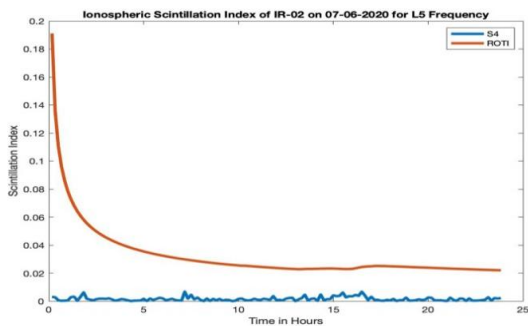


Fig. 6. Comparison of S_4 and ROTI on 2020-06-07 for IR-02 (L_5 frequency).

In Figure 6, the maximum S_4 index value of 0.0078 and the maximum ROTI index value of 0.1911 are observed. From

these, it can be concluded that no scintillations are observed on the L_5 frequency for IR-02. Figure 7 shows the correlation between S_4 and ROTI. The maximum correlation of 1 is observed many times, which is an indicative of the similarity between S_4 and ROTI.

Figure 8 shows the S_4 variations of all visible NavIC satellites on 2020-06-07 for the S_1 frequency. The maximum observed S_4 index is 0.0294 for IR-02, which is an indication of no scintillations there on 2020-06-07 for the S_1 frequency. The highest S_4 values are observed in the IR-02 satellite. Therefore, all S_4 and ROTI values are compared with the ones of the IR-02 satellite.

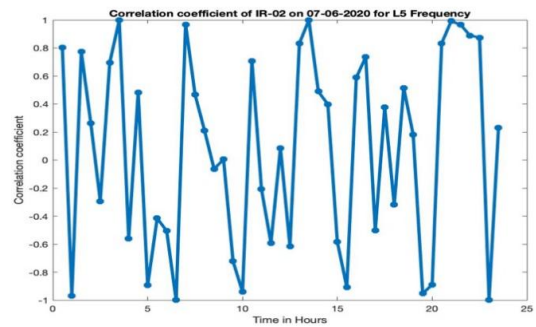


Fig. 7. Correlation of S_4 and ROTI on 2020-06-07 for IR-02 (L_5 frequency).

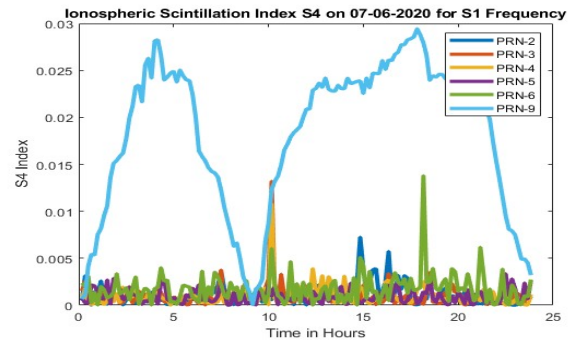


Fig. 8. S_4 amplitude variations on 2020-06-07 for S_1 frequency.

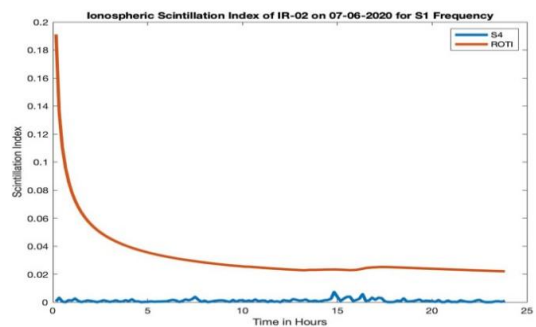


Fig. 9. Comparison of S_4 and ROTI on 2020-06-07 for IR-02 (S_1 frequency).

Figure 9 shows that the maximum S_4 index value is 0.0078 and the maximum ROTI index value is 0.1911. From this it can

be concluded that no scintillations are observed on the S_1 frequency for IR-02. Figure 10 shows the correlation between S_4 and ROTI for NavIC satellite IR-02 on 2020-06-07 on the S_1 frequency. Maximum correlation is observed many times, which indicates that ROTI can be considered as an alternative metric for the S_4 index. Figure 11 shows the skyplot of all the visible GPS and NavIC satellites at 15:00hrs of 2020-06-07 for the IGS (International GNSS Service) station which is located at Hyderabad (Lat/Long:17.417°N/78.551°E).

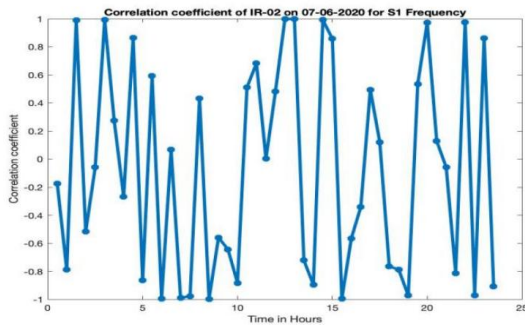
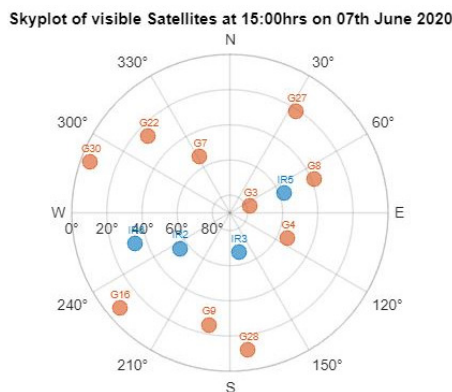


Fig. 10. Correlation of S_4 and ROTI on 2020-06-07 for IR-02 (S_1 frequency).



- Advances in Space Research*, vol. 69, no. 1, pp. 142–158, Jan. 2022, <https://doi.org/10.1016/j.asr.2021.09.026>.
- [14] Q. Li, Y. Zhu, K. Fang, and J. Fang, "Statistical Study of the Seasonal Variations in TEC Depletion and the ROTI during 2013–2019 over Hong Kong," *Sensors*, vol. 20, no. 21, Jan. 2020, Art. no. 6200, <https://doi.org/10.3390/s20216200>.
- [15] Ming O. U., Jiayan W. U., Longjiang C., and Weimin Z., "Global Ionospheric TEC and ROTI Variations during a Moderate Geomagnetic Storm," *Chinese Journal of Space Science*, vol. 41, no. 6, pp. 887–897, Nov. 2021, <https://doi.org/10.11728/cjss2021.06.887>.
- [16] X. Luo, S. Gu, Y. Lou, L. Cai, and Z. Liu, "Amplitude scintillation index derived from C/N0 measurements released by common geodetic GNSS receivers operating at 1 Hz," *Journal of Geodesy*, vol. 94, no. 2, Feb. 2020, Art. no. 27, <https://doi.org/10.1007/s00190-020-01359-7>.